Interactions of cellulose cryogels and aerogels with water and oil: Structure-function relationships

Francesco Ciuffarin, Marion Négrier, Stella Plazzotta, Michele Libralato, Sonia Calligaris, Tatiana Budtova, Lara Manzocco

Interactions of cellulose cryogels and aerogels with water and oil: structure-function relationships

Francesco Ciuffarin[1], Marion Negrier[2], Stella Plazzotta[1,*], Michele Libralato[3], Sonia Calligaris[1], Tatiana Budtova[2], Lara Manzocco[1]

[1] Department of Agricultural, Food, Environmental and Animal Sciences, University of Udine, Via Sondrio 2/A, 33100 Udine, Italy

[2] MINES Paris, PSL University, Center for Material Forming (CEMEF), UMR CNRS 7635, CS 1027, 06904 Sophia Antipolis, France

[3] Polytechnic Department of Engineering and Architecture, University of Udine, Via delle Scienze 206, 33100 Udine, Italy

[*]Corresponding author

e-mail: stella.plazzotta@uniud.it

Abstract

Food-grade porous materials, aerogels and so-called cryogels, were prepared from cellulose hydrogels obtained from solutions at increasing cellulose concentration (3, 4, 5%, w/w) by supercritical-CO_2-drying (SCD) and freeze-drying (FD), respectively. The structure depended on the applied drying technique, with aerogels showing a denser network with pores < 200 nm in diameter, a specific surface area of 370-380 m^2g^{-1}, and a porosity of 92-94%. Cryogels presented larger pores (2-5 µm diameter), much lower specific surface area (around 30 m^2g^{-1}), and higher porosity (95-96%). Water vapor adsorption by aerogels and cryogels was higher than that of neat microcrystalline cellulose. The absorption of water and oil was investigated as a function of time and at equilibrium. While water was almost immediately absorbed by both aerogels and cryogels, a much longer time was needed to reach oil absorption equilibrium. Moreover, aerogels required a longer absorption time than cryogels. Material morphology governed the kinetics of absorption; the absorption at equilibrium was directly dependent on material pore volume rather than on its morphology or material-fluid affinity. As a result, due to their lower pore volume, aerogels absorbed a lower amount of water or oil (4-8 $g_{fluid}/g_{dry\ matter}$) than cryogels (8-12 $g_{fluid}/g_{dry\ matter}$). All samples showed high fluid holding capacity (> 96%). Water absorption caused a firmness decrease, but the firmness of oil-filled materials was the same as that of the unloaded ones. This study demonstrates that food-grade cellulose aerogels and cryogels can be structurally designed by varying cellulose concentration and drying techniques to obtain controlled food fluid loading.

Keywords: porous materials; microstructure; adsorption; absorption; loading

1 Introduction

Highly porous food-grade materials can be prepared by water removal from hydrogels, the latter obtained thanks to the structuration ability of biopolymers (*i.e.*, proteins and polysaccharides). The physical structure of the final dried material strongly depends on the technology applied to remove water from the hydrogel. When freeze-drying (FD) is applied, the growth of ice crystals during the freezing step induces the concentration of polymer chains between ice crystals. After ice sublimation, the final material usually possesses large macropores, low density and low internal surface area. If the starting system is a polymer solution that is gelling under freezing, the material after ice sublimation is named "cryogel" (Lozinsky, 2018; Lozinsky et al., 2003). If the starting material is a hydrogel that is frozen, ice sublimation results in, strictly speaking, "cryostructurates" (Lozinsky, 2018; Lozinsky et al., 2003), however, they are also often called "cryogels". Alternatively, supercritical-CO_2 drying (SCD) can be applied. In this case, water in the hydrogel is substituted with a liquid miscible with CO_2, which, for food applications, is food-grade ethanol. The resulting alcogels are then dried with supercritical CO_2. The distortions in the gel network are thus theoretically minimized, and the original structure is maintained (García-González et al., 2011). The obtained materials are usually characterized by high porosity and a high internal surface area, mainly due to the presence of mesopores (2-50 nm). Such open-pore low-density nanostructured materials are defined as "aerogels" (Aegerter et al., 2011).

The unique features of bio-based cryogels and aerogels are being explored in many potential industrial fields for biomedical, environmental, cosmetic and engineering purposes (Maleki et al., 2016; Tyshkunova et al., 2022). Recently, bio-aerogels were suggested for various food applications, from delivery systems of active compounds to packaging (Manzocco, Mikkonen, et al., 2021). High potentialities of cryogels and aerogels as advanced food ingredients exploitable in the modulation of food texture and nutritional profile were also demonstrated. For example, cryogels and aerogels prepared from κ-carrageenan, vegetable fibers, and whey proteins have been used to structure both water and oil in semi-solid materials (Manzocco et al., 2017; Plazzotta et al., 2019, 2021). Hydroxypropyl methylcellulose cryogels have been proven to be effective in protecting the loaded molecules (*e.g.*, curcumin) from the harsh stomach pH, promoting their controlled release, and increasing their intestinal bioaccessibility (Chuesiang et al., 2022). Similar effects in the modulation of the digestion of the loaded bioactive molecules (*e.g.*, polyunsaturated fatty acids, phytosterols) have been also demonstrated for protein and starch aerogels (Selmer et al., 2019; Ubeyitogullari & Ciftci, 2019; Uchida et al., 2022).

Cellulose is a particularly attractive biopolymer for the preparation of food-grade cryogels and aerogels. It is the most abundant polysaccharide on the Earth, not expensive, and it can also be obtained from agro-industrial vegetable side streams, in a closed loop that avoids the generation of large quantities of waste (Pires et al., 2022). Moreover, this non-digestible carbohydrate is considered a pre-biotic, being the primary source of energy for most gut microbes and acting as a gut-protection agent (Brownlee et al., 2006; David et al., 2014).

There are two main ways to make cellulose aerogels and cryogels: one is from nanocellulose and the other is by cellulose dissolution. As nanocellulose is not in the scope of our work, only aerogels and cryogels obtained *via* cellulose dissolution will be overviewed. In this technique, the first step is the preparation of a cellulose solution. However, the majority of cellulose solvents are far from being food-grade (Liebert, 2010). One of the very few acceptable options is aqueous 7-9% NaOH. The dissolution of cellulose in NaOH-water, solution properties and materials made from them have been summarized and discussed in detail in the literature (Budtova & Navard, 2016). The dissolution of cellulose in NaOH-water occurs at sub-zero temperatures; solutions are gelling in time and gelation is faster with temperature increase. To obtain a hydrogel, NaOH is washed out by placing the cellulose-NaOH-water gel in successive water baths. As water is cellulose antisolvent, cellulose is coagulating, keeping the shape of the container in which the solution is gelled (Budtova, 2019). The obtained self-standing hydrogel can be dried *via* FD or SCD, to generate cryogels (Ciolacu et al., 2016) or aerogels (Gavillon & Budtova, 2008), respectively.

Cellulose cryogels and aerogels, due to their unique properties, can represent innovative candidates as advanced food ingredients. However, to our knowledge, the functionalities of these materials in foods have not been investigated yet.

In this study, cryogels and aerogels were prepared by FD or SCD of cellulose hydrogels obtained from cellulose-NaOH-water solutions and characterized for their structural features (SEM microstructure, BET specific surface area, porosity, pore volume, and density). Following, their interaction with common food fluids (*i.e.*, water and oil) were studied, opening a range of possible food applications for cellulose-based porous templates.

2 Materials and methods

2.1 Materials

Microcrystalline cellulose (Avicel®, pH-101, degree of polymerization 180 as declared by the manufacturer) was purchased from Sigma Aldrich. Sunflower oil was obtained from a local store. Deionized water was made with System advantage A10®, Millipore S.A.S, Molsheim, France); absolute ethanol (purity > 99%) and NaOH were purchased from Fisher Chemical.

2.2 Preparation of cellulose hydrogels, cryogels, and aerogels

Cellulose hydrogels were prepared as follows. Microcrystalline cellulose was first dried at 50 °C under vacuum for at least 2 h, pre-soaked in water for a few hours and then mixed with NaOH-water, pre-cooled at -16 °C, at 50 rpm using a mixer (Hei-Torque 100, Heidolph, Schwabach, Germany) for 2 h in a thermostatic cooling bath (Huber Compatible Control CC1, Offenburg, Germany) at -5 °C. Cellulose concentration was 3, 4, and 5 % (w/w) in 8% (w/w) NaOH-water. The obtained solutions were transparent and optically homogeneous. Around 6 mL of solution was poured into cylindrical polypropylene vials (2.7 cm in diameter) and heated at 50 °C for 2 h; in these conditions, cellulose-NaOH-water solutions are gelling (Budtova & Navard, 2016). The gels were then placed in successive water baths to dilute NaOH, as tested with pH-meter (BASIC pH meter, Denver Instrument, Bohemia, USA); the resulting material was a cellulose hydrogel at pH 7.0.

To obtain cryogels, cellulose hydrogels were frozen by immersion into liquid nitrogen (-196 °C) and freeze-dried for 72 h at -80 °C and 10 mTorr (Cryotec Cosmos, Saint-Gély-du-Fesc, France).

To obtain aerogels, water in hydrogels was first replaced by ethanol, a fluid miscible with CO_2 (Budtova, 2019): cellulose hydrogels were placed in successive water-ethanol baths with a gradual increase in ethanol concentration to completely remove water. The resulting alcogels were dried with supercritical CO_2 (homemade set-up of PERSEE Mines Paris, France); the details can be found elsewhere (Zou & Budtova, 2021). Briefly, alcogels were placed in a 1 L autoclave, pressurized at 80 bar and 37 °C and ethanol purged. Two dynamic washing steps were then performed for 1 and 2 h with a CO_2 output of 5 kg h^{-1}. In between those dynamic steps, a static mode of 2 h was used, with no CO_2 output. Finally, the system was slowly depressurized at 4 bar h^{-1} and 37 °C, and cooled down to room temperature.

The obtained dried monoliths were stored in a desiccator containing granular silica gel at room temperature until analysis.

2.3 Characterization

2.3.1 Image acquisition

Sample images were acquired using an image acquisition cabinet and a Google Pixel 6 camera (Alphabet, Mountain View, California, USA). The light was provided by a LED strip properly placed to minimize shadow and glare.

2.3.2 Morphology by Scanning Electron Microscopy (SEM)

SEM micrographs were obtained using a MAIA-3 (Tescan, Brno, Czech Republic), equipped with detectors of secondary and back-scattered electrons. The internal cross-section of the samples was coated with a 14 nm layer of platinum with a Quorum Q150T metallizer (Quorum Technologies, East Sussex, UK) to prevent the accumulation of electrostatic charges and images' defaults. The observations were performed with an acceleration voltage of 3 kV.

2.3.3 Volume variation

Sample volume was calculated as the volume of the cylinder whose diameter and height were measured by a CD-15APXR digital caliber (Absolute AOS Digimatic, Mitutoyo Corporation, Kanagawa, Japan). Volume variation (ΔV, %) during the conversion of hydrogels to cryogels or aerogels was expressed as follows (eq. 1).

$$\Delta V(\%) = \frac{V_H - V_D}{V_H} \cdot 100 \qquad \text{(eq. 1)}$$

where V_H and V_D are the volumes of the hydrogel and of the dried material (cryogel or aerogel), respectively.

2.3.4 Envelope density, porosity, and pore volume

Envelope density ($\rho_{envelope}$) was measured using the Micromeritics GeoPyc 1360 Envelope Density Analyzer (Norcross, Georgia, USA) with the DryFlo® powder as a fluid medium. Each sample was measured in 5 cycles with an applied force of 27 N. Porosity (eq. 2) and pore volume (eq. 3) were calculated from the envelope ($\rho_{envelope}$) and cellulose skeletal density ($\rho_{skeletal}$ = 1.5 g cm^{-3}, Sun, 2005):

$$Porosity\ (\%) = \left(1 - \frac{\rho_{envelope}}{\rho_{skeletal}}\right) \cdot 100 \qquad \text{(eq. 2)}$$

$$Pore\ volume\ (cm^3 g^{-1}) = \frac{1}{\rho_{envelope}} - \frac{1}{\rho_{skeletal}} \qquad \text{(eq. 3)}$$

2.3.5 Specific surface area

The specific surface area (S_{BET}) was determined by measuring N_2-adsorption isotherm at 77 K with the Micromeritics ASAP 2020 (Norcross, Georgia, USA) and using Brunauer, Emmett and Teller (BET) approach (Brunauer et al., 1938). Prior to measurements, samples were degassed 5 h at 70 °C.

2.3.6 Firmness

Firmness was measured by a uniaxial compression test using an Instron 4301 (Instron LTD., High Wycombe, UK). Samples were tested at ambient conditions using a 6.2 mm diameter cylindrical probe mounted on a 1000 N compression head at a 25 mm/min crosshead speed. Force-distance curves were obtained from the compression tests and firmness was taken as the maximum force (N) required to penetrate the sample for 2 mm.

2.3.7 Water vapor adsorption

The water vapor sorption isotherms were recorded with the ProUmid "Vsorp Basic" dynamic vapor sorption analyzer system (ProUmid, Ulm, Germany). The monoliths were cut using a microtome blade to obtain 0.4 g samples. The latter were placed in aluminium plates (86 mm in diameter) and kept in a climatic chamber at 25 ± 0.1 °C. The percentage of relative humidity (RH) in the sample headspace was automatically increased from 0 ± 0.1% RH to 90 ± 0.1% RH with 10% RH steps. The equilibrium of each step was considered to be reached when sample mass variation was lower than 0.01% for at least 300 min. The water vapor isotherms were expressed as moisture ($g_{H_2O}/g_{dry\ matter}$) as a function of sample water activity (a_w), which corresponds to RH/100 in the headspace of the sample at equilibrium conditions.

2.3.8 Water and oil absorption kinetics

Cryogels and aerogels were manually cut into cubes of 1 cm^3 volume and weighted (W_0). Cubes were immersed into Petri plates containing water or sunflower oil at room temperature (22 °C). At defined time intervals, samples were withdrawn, wiped with absorbent paper, and weighed (W_t). The experiment was carried out until a constant weight was reached (*plateau* or equilibrium value), as indicated by no weight variation in 3 consecutive measures. Absorbed water or oil at each time was expressed as the ratio between weight gain at time t (min) and the initial weight of the cryogel or aerogel sample (eq. 4).

$$Absorbed\ solvent\ \left(g_{fluid}/g_{dry\ matter}\right) = \frac{(W_t - W_0)}{W_0} \qquad \text{(eq. 4)}$$

The maximum solvent absorption capacity was taken at equilibrium.

2.3.9 Water and oil holding capacity

When the absorption reached the equilibrium, around 100-200 mg of sample (W_1) was placed into 1.5 mL microtubes and centrifuged at 15,000*g* for 30 min using a microcentrifuge (Mikro 120, Hettich Zentrifugen, Andreas Hettich GmbH and Co, Tuttlingen, Germany). After centrifugation, the released fluid was accurately wiped using absorbing paper and the sample was weighted again (W_2). Water (WHC) and oil holding capacity (OHC) were calculated as the percentage ratio between the weight of fluid retained in the sample after centrifugation and the total fluid weight initially present (eq. 5).

$$Fluid\ Holding\ Capacity\ (\%) = \frac{S \cdot W_1 - (W_1 - W_2)}{S \cdot W_1} \cdot 100 \qquad \text{(eq. 5)}$$

where *S* represents the weight fraction (%) of the fluid initially present in the sample.

2.3.10 Data analysis

Data were expressed as the mean ± standard error of at least two measurements from two experimental replicates (n ≥ 4). Statistical analysis was performed by using R v. 4.0.3 (The R Foundation for Statistical Computing). ANOVA test was used to determine statistically significant differences between means ($p < 0.05$). Bartlett's test was used to check the homogeneity of variance ($p \geq 0.05$) and the Tukey test was used as *post-hoc* test ($p < 0.05$).

3 Results and discussion

3.1 Characterization of cryogels and aerogels

Table 1 shows the visual appearance and microstructure of cryogels and aerogels prepared *via* freeze-drying (FD) and supercritical-CO_2 drying (SCD), respectively, of hydrogels obtained from cellulose solutions containing 3, 4, 5% (w/w) cellulose.

Table 1. Visual appearance and SEM microstructure of cryogels and aerogels prepared from cellulose solutions containing 3, 4, 5% (w/w) cellulose.

Samples	Cellulose concentration in the initial solution (%, w/w)		
	3	4	5
Cryogel	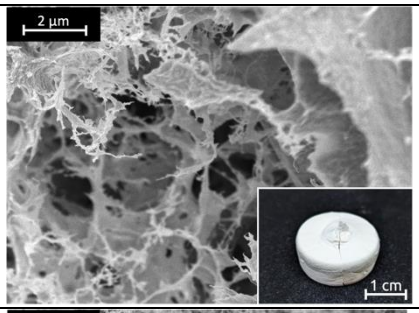	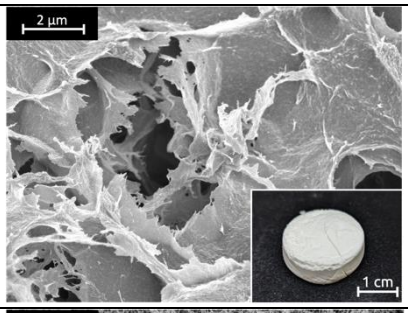	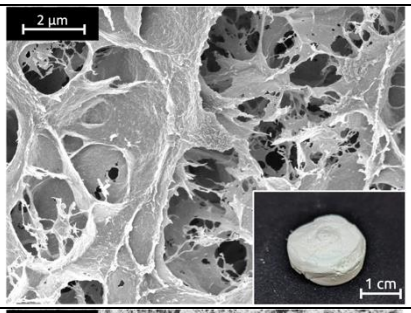
Aerogel	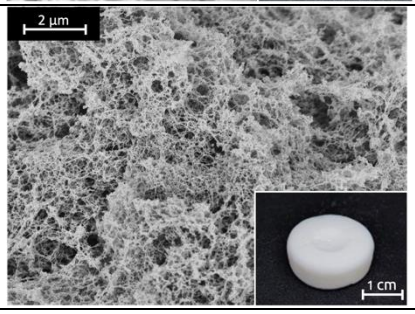	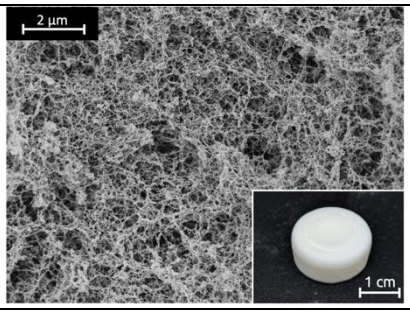	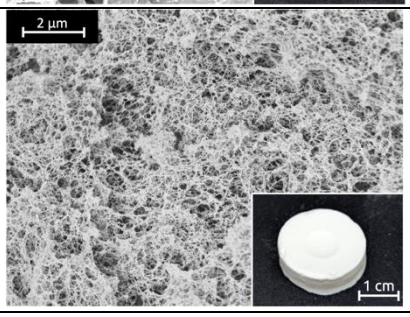

Both cryogels and aerogels appeared visually opaque (Buchtová & Budtova, 2016; Gavillon & Budtova, 2008). Cryogels showed an uneven surface with evident cracking, whereas aerogels appeared more homogeneous without visible cracks (insets in Table 1). SEM revealed significant differences between aerogel and cryogel morphology (Table 1). In cryogels, larger pores (around and below 2-5 μm) with flat walls were observed, in agreement with previous literature (Buchtová & Budtova, 2016). Although ice crystals sublimation during FD avoids liquid-vapor interfaces and thus capillary surface tension (Fricke & Tillotson, 1997), ice crystal formation and growth during hydrogel freezing force cellulose chains to locally collapse and concentrate, resulting in large pores and non-porous pore walls (Assegehegn et al., 2019). By contrast, aerogels showed a more homogeneous microstructure (Table 1), characterized by a fibrillated network, with the majority of pores of diameter lower than 200 nm.

The conversion of hydrogels into cryogels led to a slight volume increase, as indicated by the positive volume variation (Table 1). This result can be attributed to the ice crystal growth during

FD (Assegehegn et al., 2019). By contrast, aerogel preparation caused volume contraction (Table 1), which can be attributed to the increased difference in solubility parameters between cellulose (39 $MPa^{0.5}$), ethanol (26.5 $MPa^{0.5}$) and CO_2 (around 5 - 8 $MPa^{0.5}$ for the supercritical CO_2 in the conditions used in the present study) (Hansen, 2007; M. Zhang et al., 2017). As a consequence, cryogels presented lower density than the aerogels made from cellulose solutions of the same concentration (Table 2). As expected, higher cellulose concentrations in the initial solution led to both cryogels and aerogels of higher density. The porosity of both materials was higher than 90% and it was slightly lower for aerogels as compared to cryogels. The pore volume of cryogels was higher than that of aerogels, and for both types of materials pore volume decreased with density increase (Table 2).

Table 2. Volume variation, envelope density, porosity, pore volume, BET-specific surface area, and firmness of cryogels and aerogels prepared from cellulose solutions containing 3, 4, 5% (w/w) cellulose.

Sample	Cellulose solution concentration (%)	ΔV (%)	Envelope density ($g\ cm^{-3}$)	Porosity (%)	Pore Volume ($cm^3\ g^{-1}$)	S_{BET} ($m^2\ g^{-1}$)	Firmness (N)
Cryogel	3	9.5 ± 4.7 ^{b}	0.056 ± 0.002 ^{d}	96.2 ± 0.1 ^{a}	17.01 ± 0.60 ^{a}	28 ± 0 ^{b}	10.44 ± 1.1 ^{e}
	4	7.7 ± 1.8 ^{b}	0.071 ± 0.002 ^{c}	95.3 ± 0.1 ^{b}	13.40 ± 0.37 ^{b}	31 ± 2 ^{b}	19.9 ± 0.57 ^{d}
	5	4.9 ± 0.8 ^{c}	0.077 ± 0.004 ^{b}	94.9 ± 0.3 ^{b}	12.30 ± 0.64 ^{b}	30 ± 1 ^{b}	25.1 ± 0.48 ^{c}
Aerogel	3	- 25.9 ± 2.4 ^{a}	0.077 ± 0.007 ^{b}	93.8 ± 0.3 ^{c}	10.08 ± 0.57 ^{c}	384 ± 4 ^{a}	21.0 ± 0.36 ^{d}
	4	- 23.3 ± 3.2 ^{a}	0.098 ± 0.005 ^{ab}	93.5 ± 0.4 ^{cd}	9.54 ± 0.59 ^{c}	380 ± 10 ^{a}	35.8 ± 1.57 ^{b}
	5	- 20.8 ± 2.6 ^{a}	0.112 ± 0.006 ^{a}	92.9 ± 0.2 ^{d}	8.69 ± 0.21^{c}	371 ± 11^{a}	44.1 ± 1.08 ^{a}

$^{a\text{-}e}$: In the same column, mean values indicated by different letters are statistically different ($p < 0.05$).

Specific surface area (S_{BET}), which reflects the presence of mesopores and small macropores (< 200 nm), was more than 10-times higher for aerogels as compared to cryogels (Table 2), in line with SEM observations (Table 1) and results reported in the literature for bio-aerogels (Buchtová & Budtova, 2016; Zou & Budtova, 2021). It should be noted that large macropores are not detected by the BET approach, and thus a complete pore size distribution is not possible based on S_{BET} results solely (Robitzer et al., 2011; Zou & Budtova, 2021).

As a result of the lower density, cryogels presented lower firmness as compared to that of the aerogels prepared from cellulose solutions of the same concentration (Table 2). This is in line with the literature results. For instance, κ-carrageenan cryogels and aerogels showed firmness values of 1.2 and 47.1 N, respectively (Plazzotta et al., 2019); similarly, cryogels and aerogels prepared from whey protein hydrogels showed firmness of 18.5 and 29.5 N, respectively (Manzocco et al., 2021). As expected, since density increased with cellulose concentration, the

firmness followed a similar trend, similarly to the previously reported trend for the Young's modulus of various porous cellulose materials (Buchtová et al., 2019; Schestakow et al., 2016).

3.2 Interaction with water and oil

In order to analyze the capacity of cellulose cryogels and aerogels to interact with water vapor, moisture adsorption isotherms were assessed. As a representative example, Figure 1 shows data relevant to cryogels and aerogels made from 5% (w/w) cellulose solutions (density 0.077 ± 0.004 and 0.112 ± 0.006 g cm^{-3}, respectively). The adsorption isotherm of microcrystalline cellulose is shown for comparison; the results for aerogels and cryogels made from cellulose solutions of other concentrations are presented in Figure S1 of the Supporting Information.

Microcrystalline cellulose isotherm was consistent with the literature data (Portugal et al., 2010). A steady increase in the moisture content was observed in the a_w region up to 0.7, related to the saturation of hydrophilic cellulose sites. Upon further a_w increase ($a_w > 0.7$), an inflection point in the adsorption isotherm was observed, followed by higher moisture adsorption (Figure 1). This is attributed to the cleavage of cellulose intermolecular hydrogen bonds by water, which interacts with cellulose and promotes fiber swelling (Portugal et al., 2010). The transformation of microcrystalline cellulose into cryogels and aerogels did not change the form of the isotherm but resulted in a shift towards higher moisture values over the entire a_w range (Figure 1), indicating an increased ability of cellulose to interact with water vapor; the same phenomenon was recorded for aerogels and cryogels made from cellulose solutions of 3% and 4% (Figure S1). Data shown in Supplementary Figure S1 indicate no effect of cellulose concentration in the solution on the moisture uptake of both cryogels and aerogels. It is known that microcrystalline cellulose actually contains a rather high crystalline fraction, limiting the interactions with water vapor (Bhandari, 2013). The conversion of microcrystalline cellulose into cellulose II-based cryogels and aerogels decreases the crystalline fraction, thus increasing cellulose accessibility to water vapor (Yue et al., 2012).

Figure 1 also shows that the isotherms were negligibly affected by the drying technique (freeze-drying vs supercritical drying), and not influenced by material porosity or specific surface area either (Table 2).

The possibility of using cellulose cryogels and aerogels as innovative food ingredients requires the knowledge of their ability to absorb and retain the most common liquids used in foods, namely water and oil. The kinetics of water and oil absorption by aerogels and cryogels is shown in Figure 2. Upon contact with water, an extremely fast absorption was observed for all the samples (Figure 2), so that the absorption equilibrium was reached after a few seconds. The absorption of oil was from one to three orders of magnitude slower than that of water (Figure

2). The faster absorption of water as compared to oil by both cryogels and aerogels can be attributed to the hydrophilic nature of cellulose as well as to the lower viscosity of water (0.001 Pa s at 25 °C) as compared to that of sunflower oil (0.060 Pa s at 25 °C) (Lucas-Washburn equation).

Cryogels were found to absorb fluids faster than aerogels. For example, in the case of cryogels, oil absorption approached the equilibrium within 15-60 min (supplementary Figure S2), while aerogels showed a more gradual oil absorption, which leveled off only after 200-250 min. These differences in fluid absorption kinetics can be attributed to the different morphology of cryogels and aerogels. In particular, aerogels present much smaller pores as compared to cryogels, as seen in Table 1 and also deduced from the specific surface area of the materials (Table 2).

The maximum water and oil absorption values (or *plateau* values in Figure 2) of all the prepared materials were plotted as a function of material pore volume (Figure 3). These values varied from 4 to 8 $g_{fluid}/g_{dry\ matter}$ for aerogels and from 8 to 13 $g_{fluid}/g_{dry\ matter}$ for cryogels, due to different material pore volumes (see Table 2). Interestingly, all equilibrium values fell on the same linear trend ($R^2 = 0.92$; $p < 0.05$) as a function of material pore volume despite the hydrophilic nature of cellulose, and not depending on the type of liquid (oil *vs* water) or pore dimensions. This highlights the pivotal role of material pore volume on fluid uptake values at equilibrium.

The literature reports the use of porous cellulose for the absorption of various liquids. Most studies used functionalized freeze-dried cellulose II for oil absorption. After silylation (Lin et al., 2015), chemical vapor deposition (Liao et al., 2016), or plasma treatment (H. Zhang et al., 2016), absorption values were in the range from 20 to 60 $g_{oil}/g_{dry\ matter}$. Similar values were also reported for functionalized freeze-dried nanocellulose. By contrast, very few examples are known about the absorption behavior of neat cellulose II aerogels. In the study of Chin et al. (2014) cellulose coated with TiO_2 showed a five times higher oil absorption capacity (up to 28 $g_{oil}/g_{dry\ matter}$), as compared to its non-coated counterpart (5 $g_{oil}/g_{dry\ matter}$). The results acquired in this study (Figures 2 and 3) demonstrate that cellulose aerogels and cryogels absorb large quantities of water and oil without any chemical modification. This is particularly relevant for the food application of these porous materials: in fact, despite resulting in high fluid absorption, the chemical modifications cited above are not acceptable for food applications.

The effect of water and oil absorption on cryogel and aerogel firmness is reported in Figure 4, where firmness values of cryogels and aerogels prior to and after water and oil absorption are plotted against porosity. Water absorption caused a significant decrease in sample firmness as compared to the dried materials (Figure 4). Differently from water-absorbed samples, oil absorption had a negligible effect on cryogel and aerogel firmness (Figure 4). The different

effect of water and oil absorption on cryogels and aerogels firmness is probably attributable to the high hygroscopicity of cellulose, which causes the hydration of the cellulose network, weakening it, as also demonstrated for other porous materials based on vegetable fibers and proteins. By contrast, oil would simply fill the voids without significantly interacting with the polymer network (Manzocco et al., 2017; Manzocco, Plazzotta, et al., 2021).

Finally, the ability of cryogels and aerogels to retain the absorbed liquid was evaluated under centrifugal stress. All the samples showed similar ($p \geq 0.05$) high water and oil holding capacity, with values higher than 96%, independent on drying technique, material porosity and specific surface area. These results were expected for aerogels, due to the ability of small pores (Table 1) to strongly entrap the fluid. Similar oil holding capacity (OHC) values (96.3 and 83.4%), were obtained for whey protein and κ-carrageenan aerogels, which presented pore sizes around 100 and 400 nm, respectively (Manzocco et al., 2017; Manzocco, Plazzotta, et al., 2021; Plazzotta et al., 2019). Remarkably, cellulose cryogels showed much higher water and oil-holding capacity values than those reported in the literature. For example, cryogels prepared from whey proteins or κ-carrageenan showed an OHC lower than 50% (Manzocco, Plazzotta, et al., 2021; Plazzotta et al., 2019). Those cryogels possess very large pores with diameters up to 900 µm. One of the reasons for the high water and oil holding capacity of the cellulose cryogels obtained in this work might be higher capillary forces due to the rather small pore size, around 2-5 µm (Table 1).

Conclusions

Cellulose aerogels and cryogels were made via supercritical- and freeze-drying, respectively, and tested for the absorption and holding capacity of water and vegetal oil. All materials possessed very high porosity, above 90%. By varying drying techniques, materials with different morphology were obtained: aerogels had a fine ramified network with pore size below 200 nm, while cryogels presented pores of few microns and lower, and continuous flat pore walls.

The kinetics of water and oil absorption was investigated: water was absorbed by aerogels and cryogels within one minute, while oil absorption was much slower due to oil higher viscosity and hydrophobicity. Oil absorption by cryogels was much faster than by aerogels, 15-60 min *vs* 200-250 min, respectively. This phenomenon was attributed to material morphology as described above.

The maximum absorption of oil and water was proportional to material pore volume, and all experimental values fell on the same linear plot. Pore volume turned out to be the main

parameter governing fluid absorption at equilibrium, which did not depend on material morphology or fluid polarity.

Finally, the water and oil holding capacity and firmness of aerogels and cryogels, both before and after water and oil loading, were analyzed. Firmness decreased with material porosity increase, as expected. Water loading caused firmness decrease as compared to the unloaded aerogels and cryogels, while the firmness of materials filled with oil was comparable to the one with air in the pores.

These interesting results open new prospects in using cellulose aerogels and cryogels in food applications. Indeed, cellulose-based materials entrapping high amounts of water or oil can find wide applications in the food sector. On one side, their functionalities can be used to develop tailored ingredients, able to modulate food textural, sensory, and nutritional properties. On the other hand, they could represent tunable templates for structuring novel foods, including animal food analogues.

Funding

Work was carried out in the framework of COST Action CA18125 "Advanced Engineering and Research of aeroGels for Environment and Life Sciences" (AERoGELS), funded by the European Commission.

Declaration of Competing Interest

The authors declare that they have no known competing financial interests or personal relationships that could have appeared to influence the work reported in this paper.

References

Aegerter, M., Leventis, N., & Koebel, M. (2011). Aerogels handbook (Advances in Sol-Gel Derived Materials and Technologies). *Springer*, 932.

Assegehegn, G., Brito-de la Fuente, E., Franco, J. M., & Gallegos, C. (2019). The Importance of Understanding the Freezing Step and Its Impact on Freeze-Drying Process Performance. In *Journal of Pharmaceutical Sciences* (Vol. 108, Issue 4, pp. 1378–1395). https://doi.org/10.1016/j.xphs.2018.11.039

Bhandari, B. (2013). Introduction to food powders. *Handbook of Food Powders: Processes and Properties*, 1–25. https://doi.org/10.1533/9780857098672.1

Brownlee, I., Dettmar, P., Strugala, V., & Pearson, J. (2006). The Interaction of Dietary Fibres with the Colon. *Current Nutrition & Food Science*, *2*(3), 243–264. https://doi.org/10.2174/157340106778017896

Brunauer, S., Emmett, P. H., & Teller, E. (1938). Adsorption of Gases in Multimolecular Layers. *Journal of the American Chemical Society*, *60*(2), 309–319. https://doi.org/10.1021/ja01269a023

Buchtová, N., & Budtova, T. (2016). Cellulose aero-, cryo- and xerogels: towards understanding of morphology control. *Cellulose*, *23*(4), 2585–2595. https://doi.org/10.1007/s10570-016-0960-8

Buchtová, N., Pradille, C., Bouvard, J. L., & Budtova, T. (2019). Mechanical properties of cellulose aerogels and cryogels. *Soft Matter*, *15*(39), 7901–7908. https://doi.org/10.1039/c9sm01028a

Budtova, T. (2019). Cellulose II aerogels: a review. In *Cellulose* (Vol. 26, Issue 1, pp. 81–121). https://doi.org/10.1007/s10570-018-2189-1

Budtova, T., & Navard, P. (2016). Cellulose in NaOH–water based solvents: a review. In *Cellulose* (Vol. 23, Issue 1, pp. 5–55). https://doi.org/10.1007/s10570-015-0779-8

Chuesiang, P., Zhang, J., Choi, E., Yoon, I. S., Kim, J. T., & Shin, G. H. (2022). Observation of curcumin-loaded hydroxypropyl methylcellulose (HPMC) oleogels under in vitro lipid digestion and in situ intestinal absorption in rats. *International Journal of Biological Macromolecules*, *208*, 520–529. https://doi.org/10.1016/j.ijbiomac.2022.03.120

Ciolacu, D., Rudaz, C., Vasilescu, M., & Budtova, T. (2016). Physically and chemically cross-linked cellulose cryogels: Structure, properties and application for controlled release. *Carbohydrate Polymers*, *151*, 392–400. https://doi.org/10.1016/j.carbpol.2016.05.084

David, L. A., Maurice, C. F., Carmody, R. N., Gootenberg, D. B., Button, J. E., Wolfe, B. E., Ling, A. v., Devlin, A. S., Varma, Y., Fischbach, M. A., Biddinger, S. B., Dutton, R. J., & Turnbaugh, P. J. (2014). Diet rapidly and reproducibly alters the human gut microbiome. *Nature*, *505*(7484), 559–563. https://doi.org/10.1038/nature12820

Fricke, J. U., & Tillotson, T. (1997). Aerogels: production, characterization, and applications. *Thin Solid Films*, *297*(1–2), 212–223. https://doi.org/10.1016/S0040-6090(96)09441-2

García-González, C. A., Alnaief, M., & Smirnova, I. (2011). Polysaccharide-based aerogels - Promising biodegradable carriers for drug delivery systems. In *Carbohydrate Polymers* (Vol. 86, Issue 4, pp. 1425–1438). https://doi.org/10.1016/j.carbpol.2011.06.066

Gavillon, R., & Budtova, T. (2008). Aerocellulose: New highly porous cellulose prepared from cellulose-NaOH aqueous solutions. *Biomacromolecules*, *9*(1), 269–277. https://doi.org/10.1021/bm700972k

Hansen, C. M. (2007). Methods of characterization - surfaces. In *Hansen Solubility Parameters: A Users Handbook, Second Edition*. CRC Press. https://doi.org/10.1201/9781420006834

Liao, Q., Su, X., Zhu, W., Hua, W., Qian, Z., Liu, L., & Yao, J. (2016). Flexible and durable cellulose aerogels for highly effective oil/water separation. *RSC Advances*, *6*(68), 63773–63781. https://doi.org/10.1039/c6ra12356b

Liebert, T. (2010). Cellulose solvents-remarkable history, bright future. In *ACS Symposium Series* (Vol. 1033, pp. 3–54). https://doi.org/10.1021/bk-2010-1033.ch001

Lin, R., Li, A., Zheng, T., Lu, L., & Cao, Y. (2015). Hydrophobic and flexible cellulose aerogel as an efficient, green and reusable oil sorbent. *RSC Advances*, *5*(100), 82027–82033. https://doi.org/10.1039/c5ra15194e

Lozinsky, V. I. (2018). Cryostructuring of polymeric systems. Cryogels and cryotropic gel-formation: Terms and definitions. *Gels*, *4*(3), 77. https://doi.org/10.3390/gels4030077

Lozinsky, V. I., Galaev, I. Y., Plieva, F. M., Savina, I. N., Jungvid, H., & Mattiasson, B. (2003). Polymeric cryogels as promising materials of biotechnological interest. *Trends in Biotechnology*, *21*(10), 445–451. https://doi.org/10.1016/j.tibtech.2003.08.002

Maleki, H., Durães, L., García-González, C. A., del Gaudio, P., Portugal, A., & Mahmoudi, M. (2016). Synthesis and biomedical applications of aerogels: Possibilities and challenges. *Advances in Colloid and Interface Science*, *236*, 1–27. https://doi.org/10.1016/j.cis.2016.05.011

Manzocco, L., Mikkonen, K. S., & García-González, C. A. (2021). Aerogels as porous structures for food applications: Smart ingredients and novel packaging materials. In *Food Structure* (Vol. 28). https://doi.org/10.1016/j.foostr.2021.100188

Manzocco, L., Plazzotta, S., Powell, J., de Vries, A., Rousseau, D., & Calligaris, S. (2021). Structural characterisation and sorption capability of whey protein aerogels obtained by freeze-drying or supercritical drying. *Food Hydrocolloids*, *122*. https://doi.org/10.1016/j.foodhyd.2021.107117

Manzocco, L., Valoppi, F., Calligaris, S., Andreatta, F., Spilimbergo, S., & Nicoli, M. C. (2017). Exploitation of κ-carrageenan aerogels as template for edible oleogel preparation. *Food Hydrocolloids*, *71*, 68–75. https://doi.org/10.1016/j.foodhyd.2017.04.021

Pires, J. R. A., Souza, V. G. L., Gomes, L. A., Coelhoso, I. M., Godinho, M. H., & Fernando, A. L. (2022). Micro and nanocellulose extracted from energy crops as reinforcement agents in chitosan films. *Industrial Crops and Products*, *186*, 115247. https://doi.org/10.1016/j.indcrop.2022.115247

Plazzotta, S., Calligaris, S., & Manzocco, L. (2019). Structure of oleogels from κ-carrageenan templates as affected by supercritical-CO 2 -drying, freeze-drying and lettuce-filler addition. *Food Hydrocolloids*, *96*, 1–10. https://doi.org/10.1016/j.foodhyd.2019.05.008

Plazzotta, S., Jung, I., Schroeter, B., Subrahmanyam, R. P., Smirnova, I., Calligaris, S., Gurikov, P., & Manzocco, L. (2021). Conversion of whey protein aerogel particles into oleogels: Effect of oil type on structural features. *Polymers*, *13*(23). https://doi.org/10.3390/polym13234063

Portugal, I., Dias, V. M., Duarte, R. F., & Evtuguin, D. v. (2010). Hydration of cellulosesilica hybrids assessed by sorption isotherms. *Journal of Physical Chemistry B*, *114*(11), 4047–4055. https://doi.org/10.1021/jp911270y

Robitzer, M., Renzo, F. di, & Quignard, F. (2011). Natural materials with high surface area. Physisorption methods for the characterization of the texture and surface of polysaccharide aerogels. *Microporous and Mesoporous Materials*, *140*(1–3), 9–16. https://doi.org/10.1016/j.micromeso.2010.10.006

Schestakow, M., Karadagli, I., & Ratke, L. (2016). Cellulose aerogels prepared from an aqueous zinc chloride salt hydrate melt. *Carbohydrate Polymers*, *137*, 642–649. https://doi.org/10.1016/j.carbpol.2015.10.097

Selmer, I., Karnetzke, J., Kleemann, C., Lehtonen, M., Mikkonen, K. S., Kulozik, U., & Smirnova, I. (2019). Encapsulation of fish oil in protein aerogel micro-particles. *Journal of Food Engineering*, *260*, 1–11. https://doi.org/10.1016/j.jfoodeng.2019.04.016

Sun, C. (2005). True density of microcrystalline cellulose. *Journal of Pharmaceutical Sciences*, *94*(10), 2132–2134. https://doi.org/10.1002/jps.20459

Tyshkunova, I. v., Poshina, D. N., & Skorik, Y. A. (2022). Cellulose Cryogels as Promising Materials for Biomedical Applications. In *International Journal of Molecular Sciences* (Vol. 23, Issue 4). https://doi.org/10.3390/ijms23042037

Ubeyitogullari, A., & Ciftci, O. N. (2019). In vitro bioaccessibility of novel low-crystallinity phytosterol nanoparticles in non-fat and regular-fat foods. *Food Research International*, *123*, 27–35. https://doi.org/10.1016/j.foodres.2019.04.014

Uchida, J., Takahashi, Y., Katsurao, T., & Sakabe, H. (2022). One-step solvent-free synthesis of carbon dot-based layered composites exhibiting color-tunable photoluminescence. *RSC Advances*, *12*(14), 8283–8289. https://doi.org/10.1039/d2ra00312k

Yue, Y., Zhou, C., French, A. D., Xia, G., Han, G., Wang, Q., & Wu, Q. (2012). Comparative properties of cellulose nano-crystals from native and mercerized cotton fibers. *Cellulose*, *19*(4), 1173–1187. https://doi.org/10.1007/s10570-012-9714-4

Zhang, H., Li, Y., Xu, Y., Lu, Z., Chen, L., Huang, L., & Fan, M. (2016). Versatile fabrication of a superhydrophobic and ultralight cellulose-based aerogel for oil spillage clean-up. *Physical Chemistry Chemical Physics*, *18*(40), 28297–28306. https://doi.org/10.1039/c6cp04932j

Zhang, M., Dou, M., Wang, M., & Yu, Y. (2017). Study on the solubility parameter of supercritical carbon dioxide system by molecular dynamics simulation. *Journal of Molecular Liquids*, *248*, 322–329. https://doi.org/10.1016/j.molliq.2017.10.056

Zou, F., & Budtova, T. (2021). Tailoring the morphology and properties of starch aerogels and cryogels via starch source and process parameter. *Carbohydrate Polymers*, *255*, 117344. https://doi.org/10.1016/j.carbpol.2020.117344

Caption of Figures

Figure 1. Water vapor adsorption isotherms of cryogels and aerogels prepared from 5% (w/w) cellulose solution (see density and porosity values in Table 2) and microcrystalline cellulose. Error bars are not visible since smaller than the symbol size.

Figure 2. Water (A) and oil (B) absorbed by cryogels and aerogels prepared from cellulose solutions containing 3, 4, 5% (w/w) cellulose. The symbols are the same for both figures. The dashed lines are given to guide the eyes. Figure 2B magnification for cryogels in the 0-30 min range is shown in Supplementary Figure S2.

Figure 3. Maximum water and oil absorption capacity of cryogels and aerogels prepared from cellulose solutions containing 3, 4, 5% (w/w) cellulose as a function of material porosity. The dashed line is the least square approximation with $R^2 = 0.96$.

Figure 4. Firmness of cryogels and aerogels prepared from cellulose solutions containing 3, 4, 5% (w/w) cellulose prior to and after water and oil absorption as a function of porosity. The dashed lines are added as a guide for eyes.

Caption of Tables

Table 1. Visual appearance and SEM microstructure of cryogels and aerogels prepared from cellulose solutions containing 3, 4, 5% (w/w) cellulose.

Table 2. Volume variation, envelope density, porosity, pore volume, BET-specific surface area, and firmness of cryogels and aerogels prepared from cellulose solutions containing 3, 4, 5% (w/w) cellulose.

Caption of Supplementary Figures

Figure S1. Water vapor adsorption isotherms of cryogels and aerogels prepared from cellulose solutions containing 3 (A) and 4% (w/w) (B) cellulose (see density and porosity values in Table 2), and microcrystalline cellulose. Error bars are not visible since smaller than the symbol size.

Figure S2. Magnification of Figure 2B of oil absorbed by cryogels prepared from cellulose solutions containing 3, 4, 5% (w/w) cellulose. The dashed lines are given to guide the eyes.

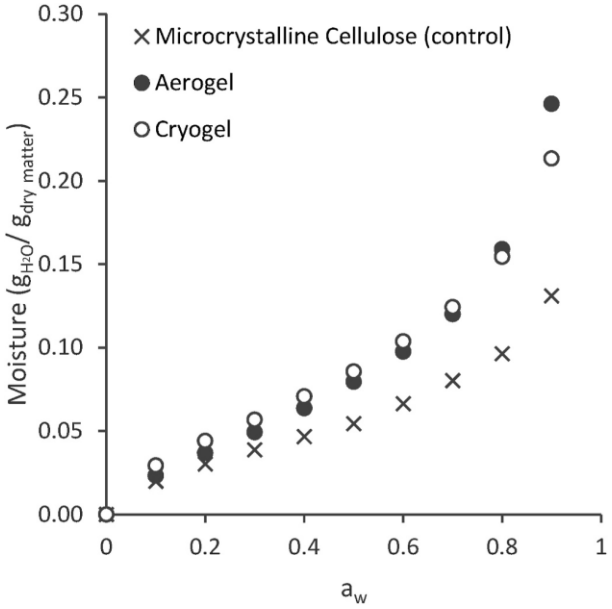

Figure 1

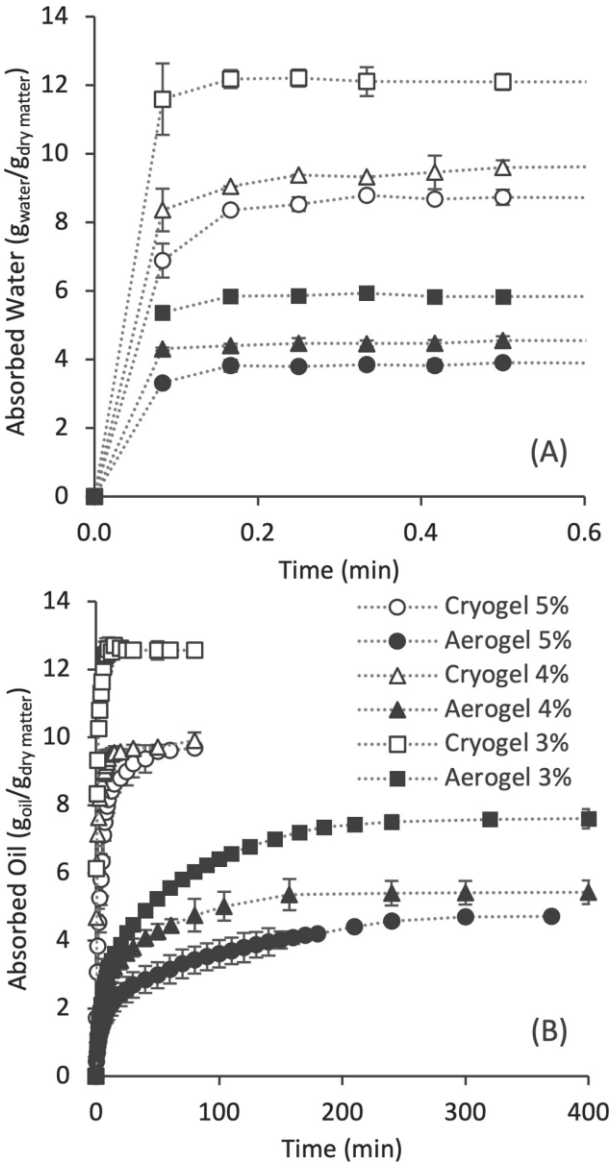

Figure 2

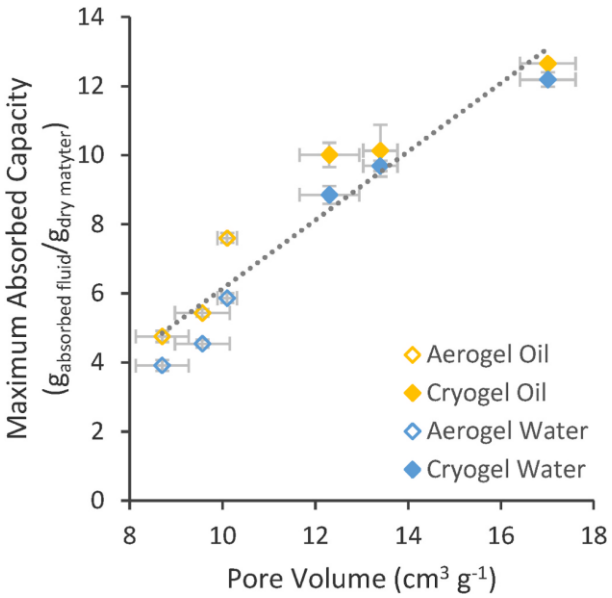

Figure 3

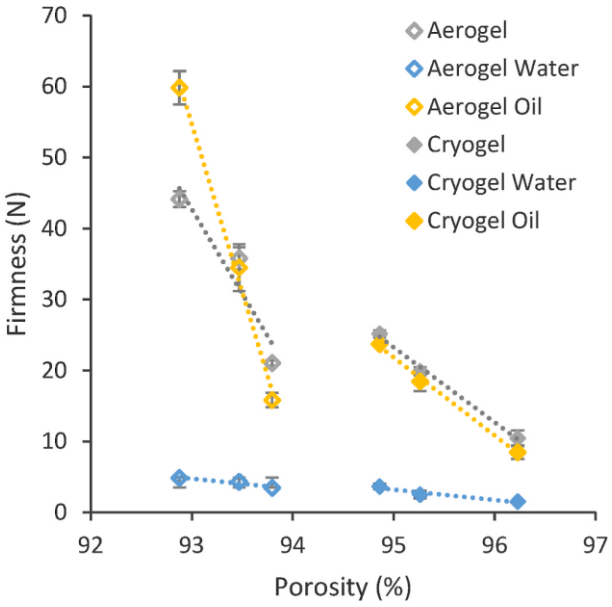

Figure 4

Figures of Supporting Information

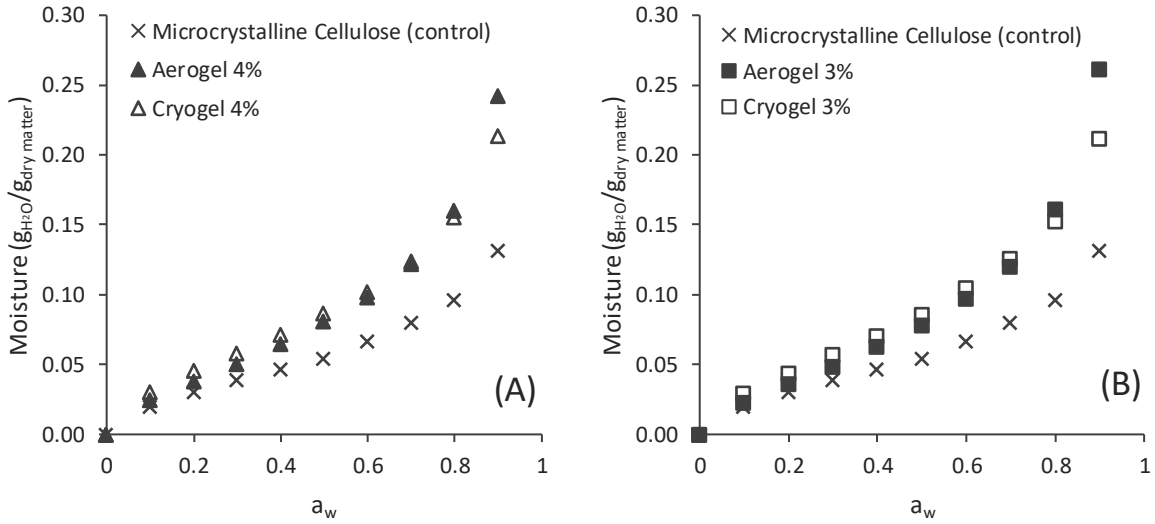

Figure S1

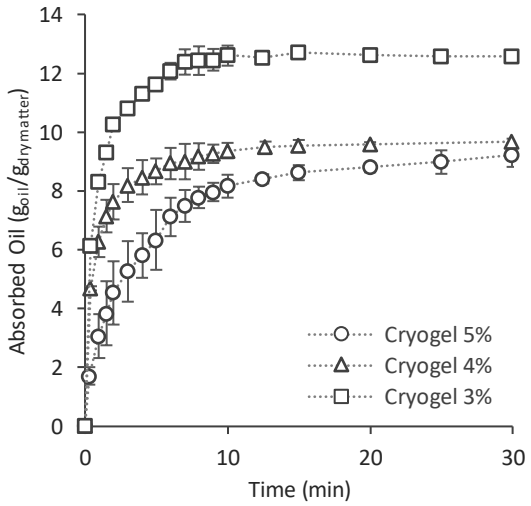

Figure S2